

1 **Digital imaging assisted geometry of chicken eggs using Hügelschäffer's model**

2

3 Valeriy G. Narushin<sup>a</sup>, Michael N. Romanov<sup>b,\*</sup>, Gang Lu<sup>c</sup>, James Cugley<sup>c</sup>, Darren K. Griffin<sup>b</sup>

4

5 <sup>a</sup> *Vita-Market Ltd, Zaporozhye, 69032, Ukraine*

6 <sup>b</sup> *School of Biosciences and School of Engineering and Digital Arts<sup>c</sup>, University of Kent,*

7 *Canterbury, Kent CT2 7NJ, UK*

8

9 \* Corresponding author. School of Biosciences and School of Engineering and Digital Arts<sup>c</sup>,

10 University of Kent, Canterbury, Kent CT2 7NJ, UK.

11 *E-mail address:* m.romanov@kent.ac.uk (M. N. Romanov)

12

## 13 **Abstract**

14 Geometrical description of the egg shape is of a great importance in a variety of studies and  
15 can be instrumental in predicting quality traits of table and hatching poultry eggs.  
16 Importantly, developments of non-destructive oomorphological models can drive novel  
17 insights in engineering and physical science and lead to new egg-related technologies and egg  
18 sorting systems for poultry industry. We attempted to test the Hügelschäffer's egg model  
19 according to which an egg profile curve can be transformed from an ellipse using a specific  
20 parameter  $w$ . For this purpose, two-dimensional digital imaging and follow-up image  
21 processing techniques of chicken eggs were employed. The formulae for recalculation of the  
22 egg volume and surface area were consequently deduced from the Hügelschäffer's equation.  
23 Eventually, we refined the Hügelschäffer's egg model and proved its applicability for  
24 defining the contours of hen's eggs. For practical use in poultry industry and food  
25 engineering, the proposed non-destructive methodology can be contributory in defining  
26 accurately the contour of any avian egg and determining such characteristics of the egg shape  
27 as volume, surface area, etc., with an expected potential in designing automated systems in  
28 poultry industry and in egg-related applications in biology, physical science, engineering and  
29 other areas.

30

31 *Keywords:* Egg quality; Non-destructive measurements; Egg volume and surface area;  
32 Hügelschäffer's model; Digital imaging; Image processing

33

## 34 **1. Introduction**

35 The basic principles of biosystems engineering are the analysis, design, and control of  
36 biologically-based systems (Alocilja, 2013). All these require an accurate and acceptable  
37 methodological foundation that would allow the implementation of analytical procedures  
38 with complex and variable biological objects. One of these objects is a poultry egg. Despite  
39 all the efforts of breeders and geneticists to breed chickens laying highly identical eggs, the  
40 variety of their shapes and sizes continues to amaze and create difficulties for scientists  
41 involved in egg-related research. These include poultry researchers focused on optimising  
42 egg incubation conditions, food scientists involved in egg processing and agricultural  
43 engineers that develop optimised technologies and equipment for egg production, incubation  
44 and processing. By virtue of an extraordinary biological diversity of the shapes and sizes of  
45 bird eggs, a specific term, oomorphology, was introduced.

46 Oomorphology has been a focal attraction and theme in biological, physical and  
47 engineering research due to the following reasons:

48 1. *Competent scientific description of a biological object.* If we manage to describe each  
49 egg with a general mathematical formula, the methodical work of researchers  
50 involved in the field of biological systematics, optimisation of technological  
51 parameters, egg incubation and selection of poultry will be greatly simplified. In this  
52 case, to distinguish one egg from another will be as simple as, say, a sphere from an  
53 ellipsoid.

54 2. *Accurate and simple determination of the physical characteristics of a biological*  
55 *object.* The external properties of the egg are extremely important for researchers and  
56 engineers who develop technologies for incubating, processing, storing and sorting  
57 eggs. Currently, the main parameter used for these purposes is the egg mass.  
58 However, in many instances, there is a need to identify and use egg volume, surface

59 area, radius of curvature and other indicators that are not difficult to measure if there  
60 is a defined mathematical formula for describing the contours of the egg.

61 3. *Biologically inspired engineering*. In terms of applications in bionics, the egg can be a  
62 suitable biological system found in nature to be studied in design of engineering  
63 systems and state-of-the-art technologies. It is not without reason that the egg-shaped  
64 geometric figure is adopted in architecture and construction as well as in shallow shell  
65 and spudcan constructions because it can withstand maximum loads with a minimum  
66 consumption of materials (Lazarus et al., 2012; Maulana et al., 2015; Zhang et al.,  
67 2017a; Zhang et al., 2017b; Zhang et al., 2019; Guo et al., 2020). Thus, the study of  
68 oomorphological parameters positively influences not only agricultural engineering  
69 and technology, but also other relevant specialties.

70 Description of avian eggs and their shapes in mathematical terms (see for review  
71 Smart, 1991) has been stirring the minds of many scholars involved not only in poultry  
72 science and ornithology, but also in engineering, architecture, construction, decoration,  
73 fashion design, vessel manufacturing, etc. If the appropriate equation were to be deduced, it  
74 would be rather straightforward to recalculate such parameters of the avian egg as its volume,  
75 surface area, curvature, and perimeter. In turn, this could give an opportunity to compare the  
76 shapes of different eggs, clutches and species defined with simple mathematical indices,  
77 which can be computerised and are easily processed within any analytical investigation.  
78 Developments of non-destructive oomorphological models assisted by such modern  
79 techniques as, for example, two-dimensional (2-D) digital imaging, have strong potential in  
80 research and industrial applications, and particularly in design of technological solutions and  
81 automated production systems including egg sorting machines.

82

83 **2. Theory**

84 *2.1. Geometry of an avian egg*

85 Most authors involved in egg geometry research have leant towards a similarity of various  
 86 avian eggs that can be described as an ellipsoid of a slightly distorted shape. Indeed, if we  
 87 consider a plane curve obtained by the normal/orthogonal projection of an avian egg, this can  
 88 be imagined as an ellipse with a shifted vertical axis along the horizontal one. Preston (1953)  
 89 was one of the first scholars to propose a modification of the ellipse equation to make it  
 90 closer to the shape of the egg. He introduced a linear formula in the parametric equation of  
 91 the ellipse. Later, Smart (1967) made this formula a bit more complicated, and Carter (1968)  
 92 modified it in such a way that a scale of the long axis of the ellipse was pulled out towards  
 93 one pole and compressed towards the other one.

94         Reviewing the studies on mathematical transformations of the ellipse equation, Köller  
 95 (2000) showed that the classic formula of an ellipse, which is

$$96 \quad \frac{x^2}{a^2} + \frac{y^2}{b^2} = 1 \quad (1)$$

97 where the parameters  $a$  and  $b$  are called lengths of axes, easily transforms into the shape of  
 98 the egg if one uses a function  $t(x)$ , by means of which each  $y$  becomes larger on the right side  
 99 and smaller on the left side, so the ellipse is transformed into a curve which resembles an egg  
 100 shape.

$$101 \quad \frac{x^2}{a^2} + \frac{y^2}{b^2} \cdot t(x) = 1 \quad (2)$$

102         Köller (2000) also proposed three simple functions  $t(x)$  for the above linear distortion  
 103 of the ellipse. These functions and the corresponding transformations of the ellipse into the  
 104 egg contour are shown in Figure 1.

105         If we consider the main dimensions of the egg contour as the length,  $L$ , and the  
 106 maximum breadth,  $B$ , so that the variables  $a$  and  $b$  from Eq. (1) are equal to

107 
$$a = \frac{L}{2} \text{ and } b = \frac{B}{2},$$

108 and apply the Köller's functions  $t(x)$ , the corresponding formulae for the egg contour can be  
 109 expressed by the following three functions:

110 1) 
$$\frac{x^2}{(L/2)^2} + \frac{y^2}{(B/2)^2} \cdot (1 + 0.2x) = 1$$

111 or

112 
$$y = \pm \frac{B}{2L} \sqrt{\frac{L^2 - 4x^2}{1 + 0.2x}} \quad (3)$$

113 2) 
$$\frac{x^2}{(L/2)^2} + \frac{y^2}{(B/2)^2 \cdot (1 - 0.2x)} = 1$$

114 or

115 
$$y = \pm \frac{B}{2L} \sqrt{1 - 0.2x} \cdot \sqrt{L^2 - 4x^2} \quad (4)$$

116 3) 
$$\frac{x^2}{(L/2)^2} + \frac{y^2}{(B/2)^2} \cdot e^{0.2x} = 1$$

117 or

118 
$$y = \pm \frac{B}{2L} \sqrt{\frac{L^2 - 4x^2}{e^{0.2x}}} \quad (5)$$

119

120 If we now represent Köller's (2000) three functions, Eqs. (3)–(5), in a graphic form  
 121 (Fig. 2), one can notice that the appropriate curves are rather similar and almost coincide  
 122 between  $x$  values of -1 and 1.

123 The Pearson correlation coefficients  $r$  between all the three functions are high: 0.953,  
 124 between  $t_1(x) = 1 + 0.2x$  and  $t_2(x) = 1/(1 - 0.2x)$ ; 0.991, between  $t_1(x) = 1 + 0.2x$  and  $t_3(x) =$   
 125  $e^{0.2x}$ ; and 0.985, between  $t_2(x) = 1/(1 - 0.2x)$  and  $t_3(x) = e^{0.2x}$ . Taking into account these high  
 126 correlations and the similarity between the three functions, let us assume that Eqs. (4) and (5)

127 give the same result as Eq. (3) and, therefore, only this function, *i.e.*, Eq. (3), may be  
 128 considered further.

129 To check if Eq. (3) is valid for an actual avian egg, it should fit the following  
 130 condition:

$$131 \quad y_{\max} = \frac{B}{2}, \quad (6)$$

132 where  $y_{\max}$  can be estimated by equating a derivative of Eq. (3) to zero; afterwards, we should  
 133 input the data of  $x$  into the obtained formula. The related mathematical calculations shown in  
 134 Supplementary Data A suggested that the transformation of the ellipse with the functions  
 135  $t_1(x)$ ,  $t_2(x)$  and  $t_3(x)$  would lead to an incorrect outcome and cannot be applied for description  
 136 of an actual egg.

137 Cook (2018) proposed a more universal function of  $t(x)$ , which is

$$138 \quad t(x) = 1 + kx, \quad (7)$$

139 where  $k$  is a coefficient that is determined experimentally depending on the shape of an actual  
 140 egg.

141 Then, the egg contour can be defined with the following equation:

$$142 \quad y = \pm \frac{B}{2L} \sqrt{\frac{L^2 - 4x^2}{1 + kx}}. \quad (8)$$

143 As was also shown by Cook (2018), for any  $k$  the width of the egg,  $B$ , corresponds to  
 144 the midpoint of the length at which  $y$  equals to 0, and that is not the maximum height of the  
 145 egg.

146 In our case,  $y_0$  can be calculated after inputting  $x=0$  into Eq. (8):

$$147 \quad y_0 = \frac{B}{2L} \sqrt{\frac{L^2 - 0}{1 + 0}} = \frac{BL}{2L} = \frac{B}{2}.$$

148 Thus, the egg breadth,  $B$ , is not the maximum value but appears at the midpoint of  $L$ , and,  
 149 therefore, Cook's formula has the same drawback as the one described by Köller (2000).

150

151 *2.2. Hügelschäffer's egg model*

152 Petrovic and Obradovic (2010) and Petrovic et al. (2011) drew attention to the scientific  
 153 heritage of the German mathematician Fritz Hügelschäffer who proposed an egg curve by  
 154 employing the process of transformation of an ellipse into an egg contour and shifting the  
 155 minor circle along the  $x$ -axis from the concentric position to the egg's blunt end by a specific  
 156 distance designated as the parameter  $w$  (as reviewed in Schmidbauer, 1948; Ferréol, 2017).  
 157 Hügelschäffer's transformation model is shown in detail in Figure 3 adopted from Petrovic et  
 158 al. (2011).

159 Petrovic and Obradovic (2010) deduced an equation for  $t(x)$ , which is defined as

$$160 \quad t(x) = 1 + \frac{2wx + w^2}{a^2}, \quad (9)$$

161 where  $w$  is the difference between the distance from the narrowed point to the maximum  
 162 breadth axis and the value of  $a$ .

163 Considering Eq. (9), the final formula for Hügelschäffer's egg contour will be as  
 164 follows:

$$165 \quad \frac{x^2}{(L/2)^2} + \frac{y^2}{(B/2)^2} \cdot \left(1 + \frac{2wx + w^2}{(L/2)^2}\right) = 1. \quad (10)$$

166 This can be rewritten in a more suitable form:

$$167 \quad y = \pm \frac{B}{2} \sqrt{\frac{L^2 - 4x^2}{L^2 + 8wx + 4w^2}}. \quad (11)$$

168 To test if the Hügelschäffer's formula has no drawbacks like other examined functions  
 169  $t(x)$  and, therefore, has no limitation to its practical use, the value of  $x = -w$ , which  
 170 corresponds to  $y_{\max}$  (Fig. 3), was put into Eq. (11):

$$171 \quad y_{\max} = \pm \frac{B}{2} \sqrt{\frac{L^2 - 4w^2}{L^2 - 8w^2 + 4w^2}} = \pm \frac{B}{2} \sqrt{\frac{L^2 - 4w^2}{L^2 - 4w^2}} = \pm \frac{B}{2}.$$



172 The obtained condition can be applied to an actual egg, so Eq. (11) is valid and useful for  
 173 empirical calculations in avian egg studies.

174 For practical use of Eq. (11), the formulae for measuring the area of the plane curve  
 175 obtained by the normal/orthogonal projection of a hen's egg,  $A$ , volume,  $V$ , and surface area,  
 176  $S$ , of an ovoid resulted from the revolution of the Hügelschäffer's egg contour, can be  
 177 recalculated as follows:

178 1. Area of the plane curve:

$$179 \quad A \approx \frac{BL^2}{9} \left( \frac{1.49}{\sqrt{L^2 - 2.667wL + 4w^2}} + \frac{2}{\sqrt{L^2 + 4w^2}} + \frac{1.49}{\sqrt{L^2 + 2.667wL + 4w^2}} + \right. \\ 180 \quad \left. + \frac{0.943}{\sqrt{L^2 - 1.333wL + 4w^2}} + \frac{0.943}{\sqrt{L^2 + 1.333wL + 4w^2}} \right). \quad (12)$$

181 2. Volume:

$$182 \quad V = \frac{\pi B^2}{256w^3} \left( 4wL(L^2 + 4w^2) - (L^2 - 4w^2)^2 \cdot \ln \left| \frac{L + 2w}{L - 2w} \right| \right). \quad (13)$$

183 Notably, the above formula is very close to the one deduced by Maulana et al. (2015)  
 184 who evaluated egg-shaped solids obtained by rotating the Hügelschäffer's egg-shaped curve  
 185 relative to the  $x$ -axis.

186 3. Surface area:

$$187 \quad S \approx \frac{\pi BL^2}{12} \left( -\frac{8BLw}{(L^2 - 4w^2)^2} + \frac{2\sqrt{3(L^2 - 2wL + 4w^2)^3 + B^2(5wL - L^2 - 4w^2)^2}}{(L^2 - 2wL + 4w^2)^2} + \right. \\ 188 \quad \left. + \frac{2\sqrt{3(L^2 + 2wL + 4w^2)^3 + B^2(5wL + L^2 + 4w^2)^2}}{(L^2 + 2wL + 4w^2)^2} + \frac{2\sqrt{(L^2 + 4w^2)^3 + 4B^2L^2w^2}}{(L^2 + 4w^2)^2} \right). \quad (14)$$

189 Detailed mathematical formulations for deducing the formulae for  $A$ ,  $V$  and  $S$ , *i.e.*,  
 190 Eqs. (12)–(14), are shown in Supplementary Data B.

191 To proceed further, the application of Eqs. (12)–(14) requires determination of the  
 192 parameter  $w$ . The latter can be found directly from an image of the investigated egg by  
 193 measuring the distance  $NC_2$  (Fig. 3). Then, the distance  $w$  would correspond to the difference  
 194 between  $NC_2$  and the half-length of the egg. However, it is rather difficult to conduct such  
 195 measurements in practice. In our preliminary study (Narushin et al., 2020) in which the 2-D  
 196 digital images of egg contours were obtained with a high-resolution camera, the egg  
 197 maximum breadth corresponded to several points on the egg surface, forming a plateau (Fig.  
 198 4). Yet, we were unable to determine the right location of the point  $C_2$  to measure the  
 199 distance  $NC_2$  correctly as its position varied within the interval 180 to 230 pixels.

200 Therefore, some theoretical attempts to simplify the procedure for the experimental  
 201 evaluation of  $w$  would be needed. For this purpose, we revised the transformation model  
 202 shown in Figure 3 implementing the following amendments: the distance  $O_wG$  equals the half  
 203 value of the egg maximum breadth,  $B/2$ ; the distance  $OD$  corresponds to the value of  $y$  in Eq.  
 204 (11) when  $x = 0$  and is indicated as  $y_0$ ; and the distance  $ON$  is the half length of the egg,  $L/2$   
 205 (Fig. 5).

206 Evaluation of  $y_0$  seems to be easier and more accurate than that of the distance  $O_wN$ .  
 207 In this case, the egg length is divided into two, and the egg diameter is measured at that point.  
 208 The value of  $y_0$  can also be defined from Eq. (11) after inputting  $x = 0$ :

$$209 \quad y_0 = \frac{BL}{2\sqrt{L^2 + 4w^2}}, \quad (15)$$

210 whence

$$211 \quad w = \frac{L\sqrt{B^2 - 4y_0^2}}{4y_0}. \quad (16)$$

212 Considering possible difficulties and complications in measuring  $y_0$ , a more universal  
 213 formula for calculating  $w$  at any point on the  $x$ -axis was deduced using Eq. (11). It was  
 214 defined that for any set of  $x$  and  $y$ :

215 
$$w_1 = \frac{\sqrt{(4x^2 - L^2)(4y^2 - B^2)}}{4y} - x, \quad (17)$$

216 
$$w_2 = -x - \frac{\sqrt{(4x^2 - L^2)(4y^2 - B^2)}}{4y}. \quad (18)$$

217 The detailed mathematical transformation of Eq. (11) is shown in Supplementary Data C.  
 218 When executing this transformation, only the upper half of the egg curve was being  
 219 considered.

220 In theory, the values of  $w$  calculated using Eqs. (17) and (18) should be valid for the  
 221 values of  $x$  for different parts of the egg curve from the point of inflection, meaning that Eq.  
 222 (17) defines the values of  $x$  at any point on the distance  $O_wN$ , while Eq. (18) determines the  
 223 values of  $x$  that correspond to any point on the distance  $O_wM$  (Fig. 5). However, this  
 224 statement needs to be verified further experimentally.

225 Previously, we suggested a method for recalculation of the egg volume and surface  
 226 area via geometrical transformation of an actual egg contour into a well-known geometrical  
 227 figure with a shape that mostly resembles the investigated egg under coequality of some of  
 228 their parameters (Narushin, 1993, 1997, 2001). Recently, we found that the method of such  
 229 transformation under the equality of the areas of plane curves of the investigated egg and its  
 230 geometrical counterpart seems to be mostly easy and accurate (Narushin et al., 2020).

231 For a validated use of the Hügelschäffer's egg contour model, Eq. (11), the defined  
 232 formula for computing the area of its projection,  $A$ , Eq. (12), should be expressed as  $B = f(A)$ .  
 233 To perform this calculation, we considered Eq. (12) as

234 
$$A = \frac{BL^2}{9} \cdot k_A, \quad (19)$$

235 where

236 
$$k_A = \frac{1.49}{\sqrt{L^2 - 2.667wL + 4w^2}} + \frac{2}{\sqrt{L^2 + 4w^2}} + \frac{1.49}{\sqrt{L^2 + 2.667wL + 4w^2}} +$$

$$237 \quad + \frac{0.943}{\sqrt{L^2 - 1.333wL + 4w^2}} + \frac{0.943}{\sqrt{L^2 + 1.333wL + 4w^2}}. \quad (20)$$

238       The above equation can be simplified by simulating the data of  $L$  and  $B$  to  $L$  ratio (*i.e.*,  
 239 shape index), which would be adequate for the variety of avian eggs, and approximating the  
 240 obtained data with a simpler dependence. To achieve a greater accuracy, we limited the  
 241 analysis to the data obtained for chicken eggs only. As the typical length of hens' eggs varies  
 242 between 5 and 7 cm and the shape index between 0.70 to 0.78 (Narushin, 1994), the  
 243 simulation of a mathematical equation was accordingly carried out by enumeration of  
 244 possibilities for the egg length range of 5 to 7 cm with the increment of 0.1 cm and for  $B/L$   
 245 with the increment of 0.01.

246       Mathematical approximation resulted in the following formula:

$$247 \quad k_A = -0.0209 \frac{B}{L} \cdot L^2 + 1.7176 = -0.0209BL + 1.7176, \quad (21)$$

$$248 \quad R^2 = 0.945.$$

249       Then,

$$250 \quad A = \frac{BL^2}{9} \cdot (-0.0209BL + 1.7176) = -0.0023B^2L^3 + 0.191BL^2, \quad (22)$$

251       whence

$$252 \quad B = \frac{41.52}{L} \left( 1 - \sqrt{1 - \frac{0.252A}{L}} \right). \quad (23)$$

253       Thus, to identify  $B$ , we should determine the area of the investigated egg,  $A$ , and egg  
 254 length,  $L$ , by direct measurements. Using these two variables, one can proceed with the  
 255 geometrical transformation of the investigated egg into the ovoid defined by Hügelschäffer's  
 256 formula and recalculate the maximum breadth,  $B_t$ , of the transformed egg following Eq. (23).  
 257 Subsequently, estimations of the egg volume and surface area can be done after inputting the  
 258 value of  $B_t$  into Eqs. (13) and (14), instead of  $B$ .

259 The objective of this study was to test the applicability of Hügelschäffer's model for  
260 digital imaging assisted estimation of egg volume and surface area in two consequent steps:

261 (1) the actual measuring of two linear variables for eggs, length and maximum  
262 breadth, and determination of the distance  $w$  using the following formulae:  $w = O_w N - L/2$   
263 and Eqs. (16)–(18); and

264 (2) comparison of the empirical data with that computed using the geometrical  
265 transformation of the egg into the ovoid if its shape is described with Hügelschäffer's formula  
266 and if the area of the egg plane curve is estimated using Eq. (23) and Eqs. (13)–(14)  
267 accordingly.

268

269 The proposed non-destructive methodology would be useful in practice for the poultry  
270 industry and food engineering to estimate accurately the contour of any avian egg as well as a  
271 number of characteristics of the egg shape like volume, surface area, circumference length,  
272 radius of curvature, area of the plane curve, etc., providing new insights in oomorphological  
273 research relevant to biology, physical science, engineering and design of automated poultry  
274 production systems.

275

### 276 **3. Materials and methods**

277 This study was based on the materials and methods as previously described by Narushin et al.  
278 (2020). Briefly, 40 fresh chicken eggs were purchased from Woodlands Farm, Canterbury  
279 and Staveley's Eggs Ltd, Coppull, UK. Each egg was weighed, and the length and maximum  
280 breadth were measured. They were also examined to directly measure their volume,  $V$ ,  
281 surface area,  $S$ , length,  $L$ , and maximum breadth,  $B$ , followed by detection of their scanned  
282 plane curves using 2-D digital imaging and subsequent image processing techniques. For this  
283 purpose, we exploited a digital camera, a non-reflection enclosure with LED (light emitting

284 diode) lighting facilities, and a personal computer. The camera (UI-2230RE) has a CMOS  
285 (Complementary Metal Oxide Semiconductor) RGB (Red, Green and Blue) imaging sensor  
286 with a resolution of 1024 (H)  $\times$  768 (V) pixels and transmits images to the computer via USB  
287 3.0 data transmission at a frame rate of 25 frames per second. This approach produced digital  
288 images of each egg. The images of the eggs were then processed using MatLab in order to  
289 compute the geometric parameters of eggs under the plane curve, *i.e.*,  $A$ ,  $L$ , and  $B$ . To convert  
290 the image dimensions in pixels into an absolute unit (cm), the measured  $L$  and  $B$  of a  
291 reference template were compared with the same variables from their digital counterparts.

292         Considering that one of the basic parameters in the Hügelschäffer's egg model is  $w$ ,  
293 the following three options for its evaluation were explored:

294         Option 1.         Estimation of the distance  $O_wN$  (Fig. 5) where the location of the point  
295  $O_w$  on the  $x$ -axis was considered to be a middle point of the plateau on the egg curve which  
296 corresponded to the maximum value of  $y$ . Using the obtained data of the distance  $O_wN$ , the  
297 parameter  $w$  was recalculated as the difference between  $O_wN$  and  $L/2$  (Fig. 5).

298         Option 2.         Estimation of the distance  $y_0$  with the subsequent recalculation of  $w$  by  
299 employing Eq. (16).

300         Option 3.         Estimation of different sets of the values of  $x$  and  $y$  on the obtained  
301 digital images with the successive recalculation of  $w$  using Eqs. (17) and (18).

302

#### 303 **4. Results and discussion**

304 The direct measurement of the 40 eggs provided values of their actual volumes  $V$ , length  $L$   
305 and maximum breadth  $B$ , and the appropriate measured egg variables including those based  
306 on 2-D digital egg images are given in Table 1. The subsequent generation of the egg images  
307 and their processing provided the other data (as analysed in detail in Narushin et al., 2020)

308 needed to examine and compare the validity of the three options for evaluating the parameter  
 309  $w$ .

310

311 **Table 1 – Data of measuring the egg variables and determining the parameter  $w$ .**

Parameters	Max. value	Min. value	Mean	Standard deviation
Length <sup>1</sup> , $L$ (cm)	6.00	5.27	5.65	0.19
Max breadth <sup>1</sup> , $B$ (cm)	4.59	4.16	4.32	0.12
Volume <sup>1</sup> , $V$ (cm <sup>3</sup> )	63.63	47.94	55.83	3.94
Parameter $w$ (cm)				
Option 1 ( $w = O_wN - L/2$ )	0.282	0.011	0.165 <sup>a</sup>	0.067
Option 2 ( $w = f(y_0)$ and Eq. (16))	0.461	0.158	0.280 <sup>b</sup>	0.100
Option 3 (Eqs. (17)–(18) and digital egg images)	0.249	0.021	0.120 <sup>c</sup>	0.050

312 <sup>1</sup>Data from Narushin et al. (2020).

313 <sup>a-c</sup> Mean  $w$  values for the three determination options with no common letters differed significantly: a, c with  $p$   
 314  $< 0.01$ ; a, b and b, c with  $p < 0.001$ .

315

316 At first, we examined Options 1 and 2 by computing the appropriate  $w$  values. As can  
 317 be seen in Table 1, the first two options for measuring  $w$  resulted in significantly different  
 318 data, and the correlation between these values was 0.130, which is too low and not clearly  
 319 showing which of the two methods of  $w$  determination is valid.

320 The recalculations of the  $w$  values by employing Eqs. (17) and (18) (Option 3)  
 321 verified our assumption to use two different formulae before and after the inflection point by  
 322 applying Eq. (17) for the  $x$  values in the  $O_wN$  interval and Eq. (18) for those in the  $O_wM$   
 323 interval (Fig. 5), on the other hand. An example of the recalculations of  $w$  for each possible  
 324 measured set of  $x$  and  $y$  is given in Figure 6.

325 Examination of the obtained data for the parameter  $w$  using the three measurement  
326 options demonstrated an essential variability of the  $w$  values, especially in the areas close to  
327 the egg ends and its middle part. Therefore, the determination of true  $w$  values turned out to  
328 be critical for conducting all further recalculations in a proper way.

329 For this purpose, we performed a graphical visualisation using the egg contours  
330 plotted for the data measured with the imaging technique and the ones recalculated with Eq.  
331 (11) when imputing different  $w$  values in the formula. A  $w$  value, which shows the full  
332 conformity of two images, should correspond to the true  $w$  value, and diagrams in Figure 7  
333 (a–c) illustrate how this process was done.

334 As shown on an example in Figure 7c, the contours of an actual single egg coincided  
335 with the recalculated egg shape if the  $w$  value for this given egg was equal to 15 px. The same  
336 procedure was applied for all the studied eggs that resulted in the following metrics of the  
337 true  $w$  parameter (Option 3): maximum value, 0.249; minimum value, 0.021; mean, 0.120;  
338 and standard deviation, 0.050 (Table 1).

339 The correlation estimates between the true  $w$  value (Option 3) and the measured ones  
340 (Table 1) were 0.439 for  $w = O_w N - L/2$  (Option 1) and 0.332 for  $w$  recalculated from Eq.  
341 (16) (Option 2). Both these estimates appeared to be too low to use for practical  
342 measurements of  $w$ . Taking into account that the way of defining the true  $w$  values that we  
343 used in this study is too tedious and time-consuming, the following amendments were put  
344 forward to address this issue.

345 It is obvious from Figure 6 that the  $w$  values are smoother within the areas near the  
346 points of  $L/4$  and  $-L/4$  on the  $x$ -axis. Based on this, the Figure 5 data were revised and  
347 modified with several additional measurements of the egg width to check which one can  
348 provide the most accurate and meaningful results for recalculating  $w$  (Fig. 8).



349 The appropriate data of egg widths ( $y_{-3L/8} \dots y_{3L/8}$  as shown in Figure 8) were taken  
 350 from the 2-D measurements based on the digital imaging that, along with the corresponding  $x$   
 351 values accordingly equal to  $-3L/8 \dots 3L/8$ , were put into Eqs. (17) and (18) for recalculating  
 352  $w$ . The obtained results are summarised in Table 2.

353

354 **Table 2 – Data of  $w$  recalculations in accordance with Figure 8 (in cm).**

Parameters	Max. value	Min. value	Mean	Standard deviation	Correlation with $w_{true}$
$w_{true}$	0.249	0.021	0.120 <sup>a</sup>	0.050	N/A
$w_{3L/8}$	0.334	0.004	0.184	0.072	0.615
$w_{L/4}$	0.296	0.010	0.170	0.062	0.659
$w_{L/8}$	0.328	0.000	0.184	0.061	0.661
$w_{-L/8}$	0.272	-0.012	0.122	0.074	0.648
$w_{-L/4}$	0.302	0.007	0.114	0.065	0.721
$w_{-3L/8}$	0.258	-0.046	0.055	0.063	0.693
Mean $w_{3L/8 \dots -3L/8}$	0.259	0.038	0.138 <sup>a</sup>	0.048	0.915
Mean $w_{L/4 \dots -L/4}$	0.274	0.022	0.142 <sup>a</sup>	0.050	0.881

355 <sup>a</sup> Mean  $w_{3L/8 \dots -3L/8}$  and  $w_{L/4 \dots -L/4}$  values did not differ significantly ( $p > 0.05$ ).

356

357 The best  $w$  prediction and the appropriate greatest correlations were found if we  
 358 consider the mean values resulting from all the measurements (Table 2). Overall, the data in  
 359 Table 2 gave the better estimation of  $w$  than the ones from Table 1. However, because  $w$   
 360 should be greater than 0, the minimum values of  $w_{L/8}$ ,  $w_{-L/8}$  and  $w_{-3L/8}$  reflected an incorrect  
 361 condition, and despite their rather high correlation with the true numbers, we discarded these  
 362 as alternative measurements for the  $w$  estimations. Because of that, the values of  $w_{L/4}$  and  $w_{-L/4}$   
 363 seemed to be more realistic having high correlation coefficients with  $w_{true}$ . The mean of  
 364 these values showed a correlation of 0.881 that was high enough for these two measurements  
 365 to be used in further calculations. Considering the appropriate two pairs of  $x$  and  $y$  (*i.e.*,  $x =$

366  $L/4$ ;  $y = y_{L/4}$  and  $x = -L/4$ ;  $y = y_{-L/4}$ ) and inputting these accordingly into Eqs. (17) and (18), we  
 367 obtained the formulae for the recalculation of  $w_{L/4}$  and  $w_{-L/4}$ :

$$368 \quad w_{L/4} = L \cdot \frac{\sqrt{3B^2 - 12y_{L/4}^2} - 2y_{L/4}}{8y_{L/4}}, \quad (24)$$

$$369 \quad w_{-L/4} = L \cdot \frac{2y_{-L/4} - \sqrt{3B^2 - 12y_{-L/4}^2}}{8y_{-L/4}}. \quad (25)$$

370 Substituting the  $w$  values in Eq. (13), we performed the calculation of egg volumes.  
 371 The egg volume was also estimated as the geometrical transformation of the investigated  
 372 eggs into the Hügelschäffer's model ovoid under the equality of their areas of the plane  
 373 curve, as above explained (see subsection 1.2. *Hügelschäffer's egg model*). The comparative  
 374 results of the egg volume estimates are presented in Table 3.

375

376 **Table 3 – Results of the calculation of the egg volume,  $V$ .**

Parameters	Mean, cm <sup>3</sup>	Correlation with $V$ measured	Standard deviation of $V$ values	Error of calculation %
$V$ , actual value	55.83 <sup>a</sup>	–	3.94	–
$V_1$ using the values of $w_{true}$	55.33 <sup>a</sup>	0.962	4.33	0.89
$V_2$ using the mean of $w_{L/4}$ and $w_{-L/4}$	55.32 <sup>a</sup>	0.962	4.32	0.91
$V_3$ using the estimates of $w = O_w N - L/2$	55.31 <sup>a</sup>	0.962	4.32	0.93
$V_4$ using the data of $A$ and $B$ (Eq. (23))	59.57 <sup>b</sup>	0.953	5.71	6.71

377 <sup>a, b</sup> Mean  $V$  values with no common letters differed significantly ( $p < 0.01$ ).

378

379 These results showed the greatest correlation coefficient (0.962) and the least  
 380 calculation error ( $< 1\%$ ) for the egg volume estimates  $V_1$ ,  $V_2$  and  $V_3$ , meaning that the

381 recalculation accuracy and congruity for the measured parameter  $w$  based on estimates of  $V_1$ ,  
 382  $V_2$  and  $V_3$  were better than  $V_4$  evaluated on the basis of the area of the plane curve. That could  
 383 be explained by the fact that Hügelschäffer's formula describes the egg shape more  
 384 accurately, thus the geometrical transformation is not needed. While conducting the  
 385 transformation procedure, calculation and measurement errors are accumulated due to the  
 386 approximate nature of Eqs. (12) and (23) as well as the conversion of square pixels into  
 387 square cm, which was shown to be more inaccurate than that for the linear transformation.

388 Overall, the results for the volume estimations by means of both measuring and/or  
 389 recalculating of  $w$  appeared to be sufficiently accurate and almost the same for all methods.  
 390 The least calculation error was observed if the values  $w_{true}$  were used, however the  
 391 appropriate mean differences relative to all other  $w$  values were insignificant (Table 3).  
 392 Therefore, we would suggest that the use of any tested method of  $w$  estimation is acceptable  
 393 for both industrial and analytical applications.

394 The recalculations of the surface area of the investigated eggs using Eq. (14) using the  
 395 same variables as for the volume estimations are shown in Table 4.

396

397 **Table 4 – Results of calculation of the egg surface area,  $S$ .**

Parameters	Mean $\pm$ SD, cm <sup>2</sup>
$S_1$ using the values of $w_{true}$	60.68 $\pm$ 3.27 <sup>a</sup>
$S_2$ using the mean of $w_{L/4}$ and $w_{-L/4}$	60.57 $\pm$ 3.27 <sup>a</sup>
$S_3$ using the estimates of $w = O_w N - L/2$	60.42 $\pm$ 3.24 <sup>a</sup>
$S_4$ using the data of $A$ and $B$ (Eq. (23))	62.83 $\pm$ 3.69 <sup>b</sup>

398 <sup>a, b</sup> Mean  $S$  values with no common letters differed significantly ( $p < 0.01$ ).

399

400 As there is no direct method for accurately measuring the egg surface area, it is  
 401 difficult to state which  $S$  from Table 4 is the most adequate and true. However, previously we

402 provided theoretical deliberations suggesting that the validity of the computed egg surface  
403 area depends on the accuracy of the appropriate formula for estimating the egg volume,  $V$   
404 (Narushin et al., 2020). The estimated values of  $S$  have similar variations as those for the  
405 calculated  $V$  (Table 3), therefore we could suggest that any way to determine the surface area  
406 would have the same drawbacks and advantages as methods for estimating the egg volume.

407 In the light of our findings, we can note some new concepts relevant to research and  
408 applications in biology, physical science, engineering and poultry industry that can be  
409 potentially based on the proposed non-destructive, digital imaging assisted oomorphology  
410 model. First, we have developed a theoretical approach to assess the adequacy of  
411 mathematical equations for evaluating the avian egg geometry including egg shape. Given the  
412 extraordinary number of such equations, with a persistent interest in their creation for almost  
413 two centuries, our approach enabled many of them to be rejected, as they do not comply with  
414 the principles of stability of the shape of the geometric figure. On the basis of this approach,  
415 the Hügelschäffer's model was selected as an equation that completely meets the basic  
416 principles and requirements for a comprehensive egg shape description. Using the exact  
417 description of the geometric shape of the eggs, the principles of a common engineering  
418 method known as Finite Element Analysis (FEA) have been developed and widely used to  
419 study the strength properties of the shell (Coucke et al., 1998; Nedomová et al., 2009; Perianu  
420 et al., 2010; Sellés et al., 2019).

421 Second, we have carried out a thorough study using a sophisticated digital imaging  
422 hardware that made it possible to develop a technique for measuring the parameter  $w$  (vertical  
423 axis shift) needed for applying Hügelschäffer's model. We described in detail all the  
424 problems that can be encountered as a result of this measurement, even when using such a  
425 methodological approach as computer scanning of egg contours.

426 Third, even for well-known geometric figures, e.g., ellipse, it is difficult to derive  
427 basic geometric formulas. To date, researchers have not come to an agreement and unified  
428 approach for determining the surface area of an ellipsoid. In our work, we demonstrated a  
429 new geometric figure, an ovoid built on the basis of the Hügelschäffer's model, for which all  
430 the previous attempts to describe it comprehensively were reduced only to inferring the  
431 formula for its volume, and even that without direct reference to the egg. In this regard, our  
432 successful derivation of the main mathematical formulas for this new geometric object can be  
433 certainly considered, in our opinion, not only as an interesting mathematical exercise but  
434 rather as an innovative work on a fully-fledged theoretical study of a new geometric body.

435 We suggest that the theoretical findings and digital imaging assisted tests we have  
436 reported here can be further incorporated in developing egg-related non-destructive  
437 technologies and automated systems applicable in research and industry.

438

## 439 **5. Conclusions**

440 Our analysis has demonstrated the validity of Hügelschäffer's formula for defining digital  
441 imaging assisted oomorphology including the contours of the hens' eggs and recalculating  
442 their geometrical variables. To tailor Hügelschäffer's model, we would recommend defining  
443 the value of the parameter  $w$  for each investigated egg. In industrial applications of such a  
444 technology, a machine vision technique can be of a great advantage. From a practical  
445 viewpoint, the measurement of linear egg parameters is a more straightforward process than,  
446 for instance, determination of the egg surface area. For laboratory use, egg images can be  
447 easily processed with Photoshop-like software or even less sophisticated programs (*e.g.*, MS  
448 Paint). Measurements of the parameter  $w$  can also be performed using a modified caliper  
449 (Smart, 1991). Even such a simple measurement using a ruler and a printed version of the  
450 image can be employed, too. Considering the simplicity and accuracy of the proposed

451 method, it would also be worthwhile to test its applicability and validity for measuring eggs  
452 of other avian species, especially those with shapes that differ from the chicken egg profile. If  
453 Hügelschäffer's egg model were to be suitable for other species, this would deliver a novel  
454 research instrument for ornithological, especially oological studies. The proposed non-  
455 destructive methodology is practically ideal in the poultry industry and food engineering  
456 areas for an accurate representation of the contour of any avian egg and can also be easily  
457 used for the exploration of such characteristics of the egg shape as volume, surface area,  
458 circumference length, radius of curvature, area of the plane curve, etc. Based on the proposed  
459 digital imaging assisted egg geometry model, we expect it will have great potential in  
460 applications for designing automated systems in the poultry industry and in egg-related  
461 research in biology, physical science, engineering and other disciplines.

462

#### 463 **Declaration of Competing Interest**

464 The authors declare no competing financial interest.

465

#### 466 **Acknowledgements**

467 We acknowledge the financial support of this work via a University of Kent internal research  
468 grant sponsored by the Global Challenges Research Fund (GCRF) Partnership Fund.

469

#### 470 **Supplementary data.**

471 Supplementary data A, B, C to this article can be found online at

472

#### 473 **References**

- 474 Alocilja, E. C. (2013). *Principles of Biosystems Engineering*.  
475 [https://www.egr.msu.edu/~alocilja/Teaching/Principles%20of%20BE%20Book%208-](https://www.egr.msu.edu/~alocilja/Teaching/Principles%20of%20BE%20Book%208-12-2013.pdf)  
476 [12-2013.pdf](https://www.egr.msu.edu/~alocilja/Teaching/Principles%20of%20BE%20Book%208-12-2013.pdf). Accessed on 6 April 2020.
- 477 Carter, T. C. (1968). The hen's egg: a mathematical model with three parameters. *British*  
478 *Poultry Science*, 9(2), 165–171.
- 479 Cook, J. D. (2018). *Equation to Fit an Egg*.  
480 <https://www.johndcook.com/blog/2018/04/18/equation-to-fit-an-egg/>. Accessed on 6  
481 April 2020.
- 482 Coucke, P., Jacobs, G., Sas, P., & De Baerdemaeker, J. (1998). Comparative analysis of the  
483 static and dynamic mechanical eggshell behaviour of a chicken egg. In *Proceedings of*  
484 *the 23rd International Conference on Noise and Vibration Engineering* (pp. 1469–  
485 1474). Leuven, Belgium.
- 486 Ferréol, R. (2017). *Hügelschäffer egg*.  
487 <http://www.mathcurve.com/courbes2d.gb/oeuf/oeuf.shtml>. Accessed on 6 April 2020.
- 488 Guo, S., Zhuang, H., Tang, W.-X., Liu, Q., & Wang, Y.-Y. (2020). Design of a bionic  
489 spudcan and analysis of penetration and extraction performances for jack-up platform.  
490 *China Ocean Engineering*, 34(1), 80–88.
- 491 Köller, J. (2000). *Egg Curves and Ovals*. [http://www.mathematische-](http://www.mathematische-basteleien.de/eggcurves.htm)  
492 [basteleien.de/eggcurves.htm](http://www.mathematische-basteleien.de/eggcurves.htm). Accessed on 6 April 2020.
- 493 Lazarus, A., Florijn, H. C. B., & Reis P. M. (2012). Geometry-induced rigidity in  
494 nonspherical pressurized elastic shells. *Physical Review Letters*, 109(14), 144301.
- 495 Maulana, A. R., Yunus, M., & Sulistyaningrum, D. R. (2015). The constructions of egg-  
496 shaped surface equations using Hugelschaffer's egg-shaped curve. *Indonesian Journal*  
497 *of Physics*, 26(2), 26–30.
- 498 Narushin, V. G. (1993). New indestructive methods of egg parameters and eggshell quality  
499 determination. In *5th European Symposium on the Quality of Eggs and Egg Products*  
500 (Vol. 2, pp. 217–222). Tours, France.

- 501 Narushin, V. G. (1994). Express method for determination of egg morphological parameters.  
502 In *Proceedings of 9th European Poultry Conference* (Vol. 1, pp. 385–386). Glasgow,  
503 UK.
- 504 Narushin, V. G. (1997). The avian egg: geometrical description and calculation of  
505 parameters. *Journal of Agricultural Engineering Research*, 68(3), 201–205.
- 506 Narushin, V. G. (2001). AP—Animal Production Technology: Shape geometry of the avian  
507 egg. *Journal of Agricultural Engineering Research*, 79(4), 441–448.
- 508 Narushin, V. G., Lu, G., Cugley, J., Romanov, M. N., & Griffin, D. K. (2020). A 2-D  
509 imaging-assisted geometrical transformation method for non-destructive evaluation of  
510 the volume and surface area of avian eggs. *Food Control*, 112, 107112.  
511 <https://doi.org/10.1016/j.foodcont.2020.107112>.
- 512 Nedomová, Š., Trnka, J., Dvořáková, P., Buchar, J., & Severa, L. (2009). Hen's eggshell  
513 strength under impact loading. *Journal of Food Engineering*, 94(3–4), 350–357.
- 514 Perianu, C., De Ketelaere, B., Pluymers, B., Desmet, W., DeBaerdemaeker, J., & Decuyper,  
515 E. (2010). Finite element approach for simulating the dynamic mechanical behaviour  
516 of a chicken egg. *Biosystems Engineering*, 106(1), 79–85.
- 517 Petrovic, M., & Obradovic, M. (2010). The complement of the Hugelschaffer's construction  
518 of the egg curve. In *2nd International Scientific Conference MonGeometrija 2010* (pp.  
519 520–531). Vlasina, Serbia.
- 520 Petrovic, M., Obradovic, M., & Mijailovic, R. (2011). Suitability analysis of Hugelschaffer's  
521 egg curve application in architectural and structures' geometry. *Buletinul Institutului*  
522 *Politehnic din Iasi: Secția Construcții de mașini*, 57(3), 115–122.
- 523 Preston, E. W. (1953). The shapes of birds' eggs. *Auk*, 70(2), 160–182.
- 524 Recktenwald, G. W. (2000). *Numerical Methods with MATLAB: Implementations and*  
525 *Applications*. Upper Saddle River, New Jersey: Prentice Hall.



- 526 Schmidbauer, H. (1948). Eine exakte Eierkurvenkonstruktion mit technischen Anwendungen.  
527 *Elemente der Mathematik*, 3(3), 67–68.
- 528 Sellés, A. G., Marcè-Nogué, J., Vila, B., Pérez, M. A., Gil, L., Galobart, À., & Fortuny, J.  
529 (2019). Computational approach to evaluating the strength of eggs: Implications for  
530 laying in organic egg production. *Biosystems Engineering*, 186, 146–155.
- 531 Smart, I. H. M. (1967). The curve of the avian egg. *Journal of Anatomy*, 101(3), 634–635.
- 532 Smart, I. H. M. (1991). Egg-shape in birds. In D. C. Deeming, & M. W. J. Ferguson (Eds.), *Egg*  
533 *incubation: its effects on embryonic development in birds and reptiles* (pp. 101–116).  
534 Cambridge, UK: Cambridge University Press.
- 535 Zhang, J., Tan, J., Tang, W., Zhao, X., & Zhu, Y. (2019). Experimental and numerical collapse  
536 properties of externally pressurized egg-shaped shells under local geometrical imperfections.  
537 *International Journal of Pressure Vessels and Piping*, 175, 103893.
- 538 Zhang, J., Zhu, B., Wang, F., Tang, W., Wang, W., & Zhang, M. (2017a). Buckling of prolate egg-  
539 shaped domes under hydrostatic external pressure. *Thin-Walled Structures*, 119, 296–303.
- 540 Zhang, J., Wang, M., Wang, W., Tang, W., & Zhu, Y. (2017b). Investigation on egg-shaped pressure  
541 hulls. *Marine Structures*, 52, 50–66.
- 542

543 **Figure captions**

544 **Fig. 1.** – Transformation of an ellipse into an egg contour with the three different functions  $t(x)$  (adopted  
545 from Köller, 2000).

546 **Fig. 2.** – Curves of the three Köller's (2000) egg contour functions:  $t_1(x) = 1 + 0.2x$  (green triangles);  $t_2(x) =$   
547  $1/(1 - 0.2x)$  (dark blue diamonds) and  $t_3(x) = e^{0.2x}$  (red circles).

548 **Fig. 3.** – Hügelschäffer's transformation of an ellipse into an egg contour (from Petrovic et al., 2011).

549 **Fig. 4.** – Digital egg contour based on the data of Narushin et al. (2020).

550 **Fig. 5.** – Estimation of the parameter  $w$  by measuring  $y_0$  on the basis of the amended Hügelschäffer's egg  
551 model.

552 **Fig. 6.** – Recalculation of  $w$  (in pixels) with Eqs. (17) and (18) using the data of scanning the egg images,  
553 where the range of  $x$  values reflects the egg length,  $L$ , and the range of  $y$  values the egg maximum  
554 breadth,  $B$ .

555 **Fig. 7.** – An example of graphical visualisation of the egg contours (all dimensions are given in pixels): (a)  
556 A diagram plotted for the data of egg imaging. (b) A brown line corresponds to the egg shape calculated  
557 with Eq. (11) and  $w=45$  and is plotted relative to the egg contour (blue line) measured using machine  
558 vision. (c) The both lines of the actual egg shape (blue) and the recalculated one (brown) coincided when  
559  $w=15$ .

560 **Fig. 8.** – Amended measurements of the egg width along its longitudinal axis for recalculation of  $w$ .

561

Figure 1

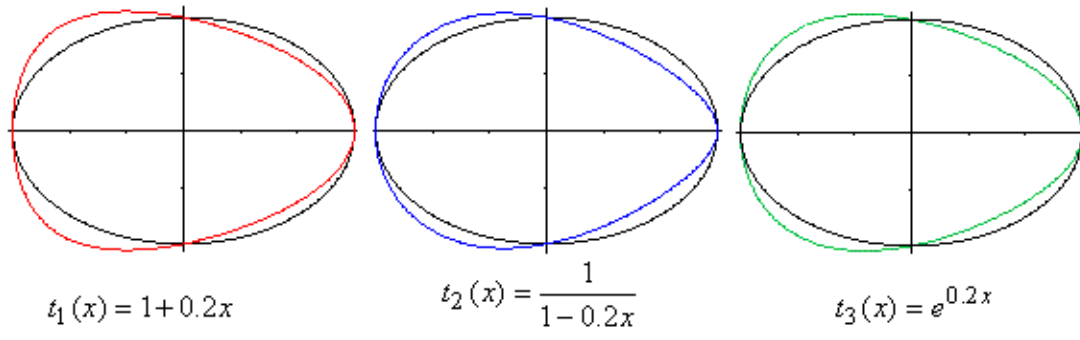


Figure 2

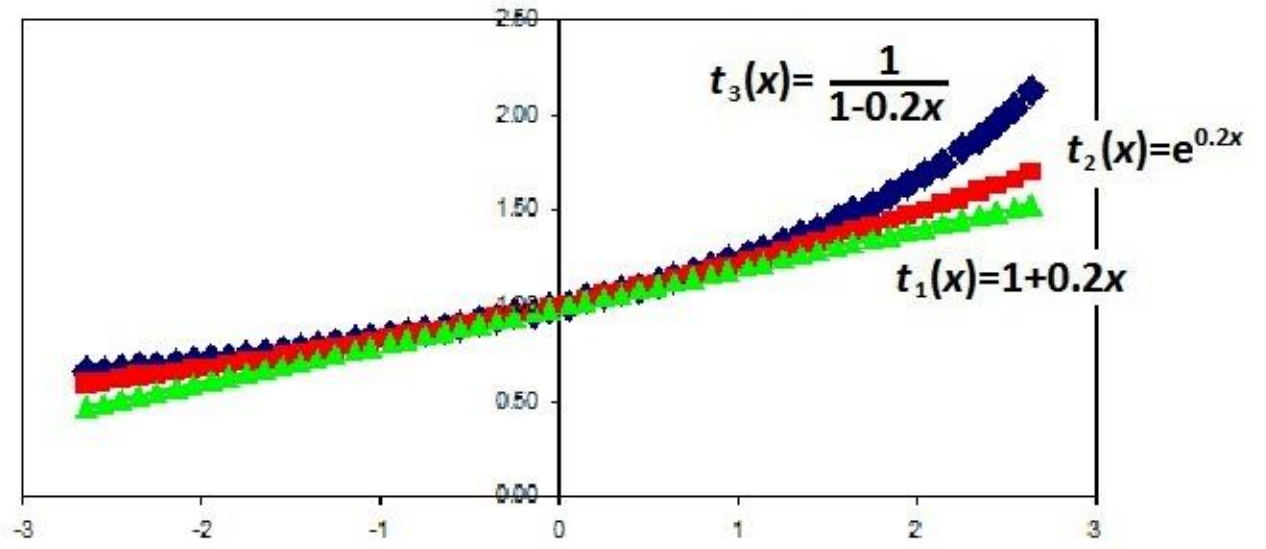


Figure 3

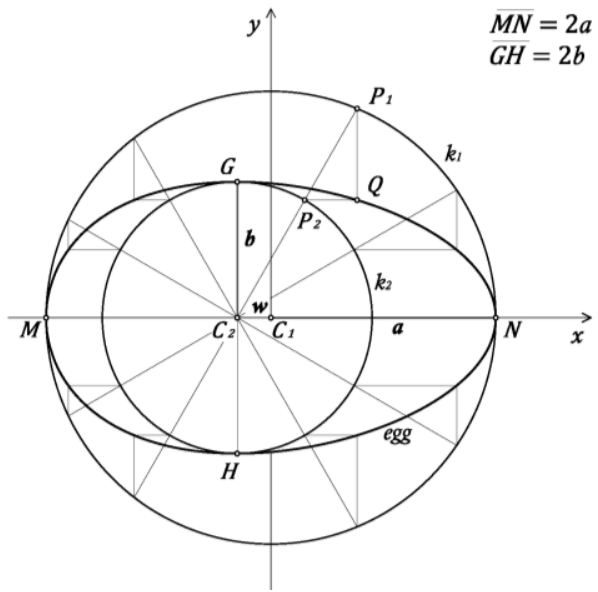


Figure 4

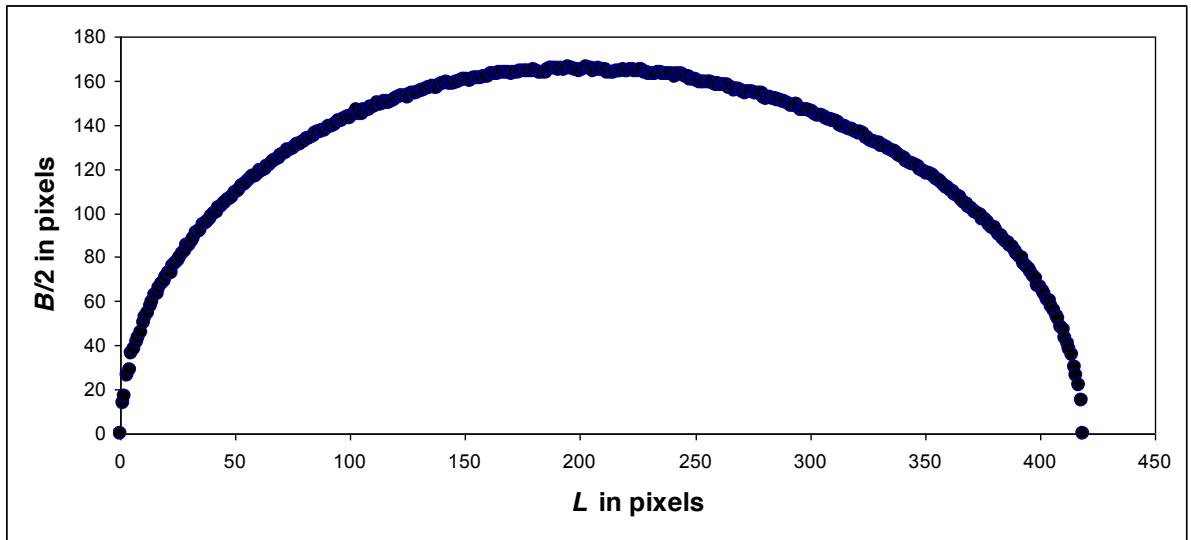


Figure 5

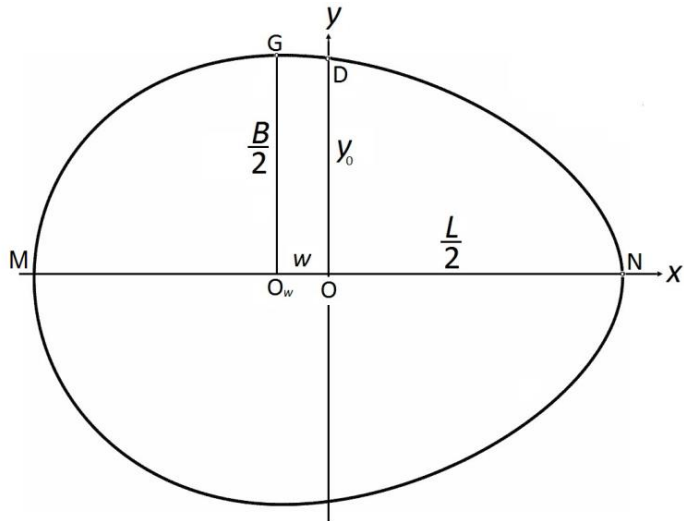


Figure 6

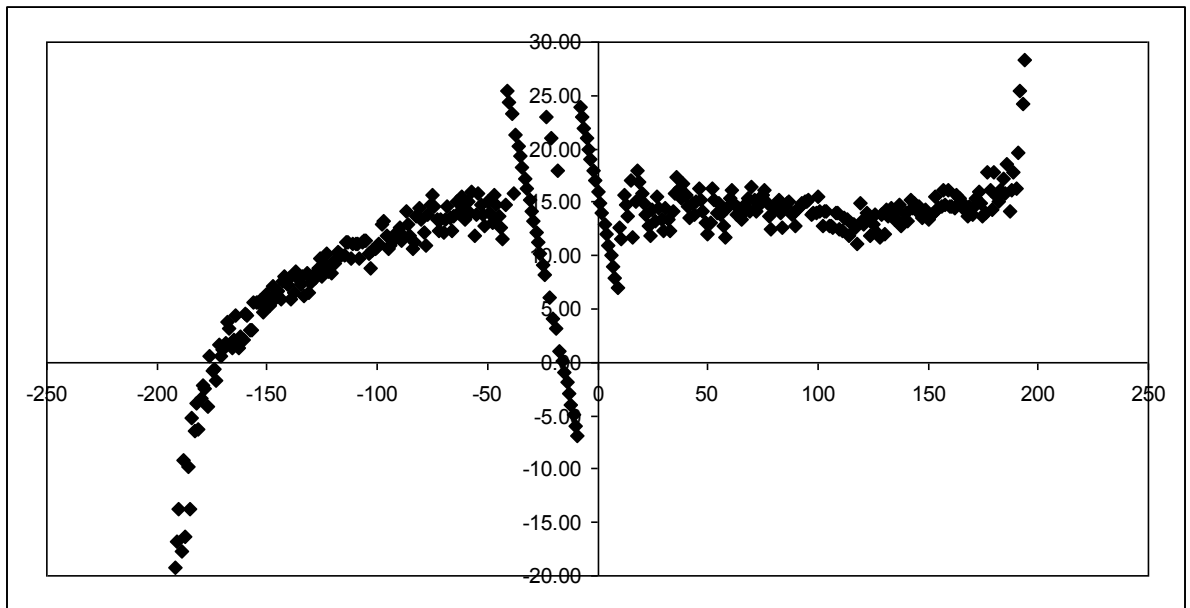
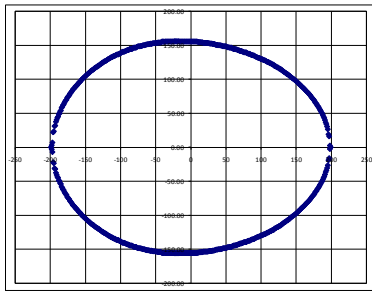


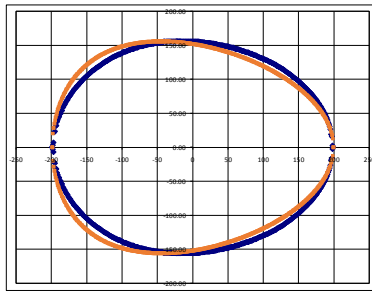


Figure 7

(a)



(b)



(c)

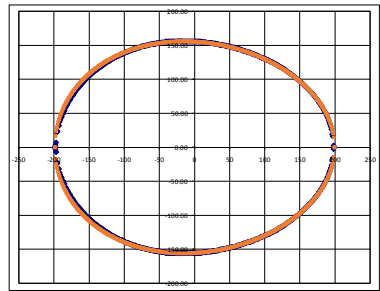


Figure 8

